Whole organic electronic synapses for dopamine detection

Martina Giordani[a], Michele Di Lauro[a], Marcello Berto[a], Carlo A. Bortolotti[a,b], Dominique Vuillaume[c], Henrique L. Gomes[d,e], Michele Zoli[f] and Fabio Biscarini[a*]

[a] Life Sciences Department, Università di Modena and Reggio Emilia, Via Campi 103, 41125 Modena, Italy; [b] National Research Council, CNR-NANO, Via Campi 213/a, 41125 Modena, Italy; [c] Institute for Electronics Microelectronics and Nanotechnology, CNRS and University of Lille, Av. Poincaré, F-59652cedex, Villeneuve d'Ascq, France; [d] Universidade do Algarve, FCT, Campus de Gambelas, Faro, Portugal; [e] Instituto de Telecomunicações, Av. Rovisco Pais, Lisboa, Portugal; [f] Department of Biomedical, Metabolic, and Neural Sciences, Center for Neuroscience and Neurotechnology, Università di Modena e Reggio Emilia, Via Campi 287, 41125 Modena, Italy

ABSTRACT

A whole organic artificial synapse has been fabricated by patterning PEDOT:PSS electrodes on PDMS that are biased in frequency to yield a STP response. The timescale of the STP response is shown to be sensitive to the concentration of dopamine, DA, a neurotransmitter relevant for monitoring the development of Parkinson's disease and potential loco-regional therapies. The sensitivity of the sensor towards DA has been validated comparing signal variation in the presence of DA and its principal interfering agent, ascorbic acid, AA. The whole organic synapse is biocompatible, soft and flexible, and is attractive for implantable devices aimed to real-time monitoring of DA concentration in bodily fluids. This may open applications in chronic neurodegenerative diseases such as Parkinson's disease.

Keywords: organic bioelectronics, PEDOT:PSS, STP, synapse, dopamine

* Prof. Fabio Biscarini Ph.D FRSC; email: fabio.biscarini@unimore.it

1. INTRODUCTION

Organic bioelectronics is emerging as a robust and versatile platform for biosensing and transduction of biofunctional signals[1–4]. In this context a new class of devices mimicking the electrical behavior of physiological synapses has recently been developed: the Organic Synapstor. Being one of the firstly evolved logical elements in animals (they are present even in the phylogenetically ancient phylum of Cnidaria[5]), synapses have the function of transmitting action potentials (i.e. ionic currents) between two subsequent neurons in a neural network and modulate their intensity, in order to convey information in a controlled manner. In the synapse the action potential coming from the pre-synaptic neuron is transformed into the release of neurotransmitters (viz. glutamate, serotonin, noradrenaline, among others) that targets the post-synaptic neuron. Because in each synapse there is a finite amount of neurotransmitters available, they need to be recovered after the discharge. This recovery occurs in a characteristic time τ: if the spiking frequency (f) is lower than τ^{-1} the neurotransmitters have enough time to recover, hence will be released in equal (or even larger) quantity at the arrival of the following spike (facilitating behavior); on the contrary if f is larger than τ^{-1} the second spike will reach the

Organic Sensors and Bioelectronics IX, edited by Ioannis Kymissis, Ruth Shinar, Luisa Torsi, Proc. of SPIE Vol. 9944, 99440P · © 2016 SPIE
CCC code: 0277-786X/16/$18 · doi: 10.1117/12.2239532

synapses before the neurotransmitters have had their time to recover, hence they will be released in lower amount (depressing behavior). The combination of facilitating and depressing behaviors is called short-term plasticity (STP).

In order to mimic STP-like response, an electronic device needs to rely on RC (resistance-capacitance) elements. Just like synapses, RC circuits show a characteristic relaxation time (i.e. a characteristic stimulus frequency), and exhibit frequency dependence of the displacement current magnitude. STP response in organic electronic devices was demonstrated by Alibart et al. in 2010 with the NOMFET (Nanoparticle Organic Memory Field-Effect transistor)[6] obtained by embedding gold nanoparticles in the semiconductor channel of a pentacene thin film transistor. The STP response arises from a network of capacitances (the nanoparticles) interconnected through the resistive pentacene channel. Also liquid-gated devices, analogues of NOMFETs, EGOSs (Electrolyte-Gated Organic Synapstors), were recently demonstrated[7,8]. These devices rely also on the high capacitance of the electrical double layer that builds up at the interfaces between each electrode and the electrolyte: when the double layer is perturbed, a displacement current arises and its intensity is modulated by the frequency of the perturbation.

In this work we show a whole organic artificial synapse, made of two electrodes made of the conductive polymer PEDOT:PSS (poly-3,4-ethylene-di-oxy-thiophene:polystyrene sulphonate), directly patterned through laser ablation onto a soft and flexible PDMS (poly-di-methyl-siloxane) substrate. Upon biasing one of the electrodes with voltage pulses, the displacement current exhibits STP response. The characteristic time arises from the large capacitance of the interface between PEDOT:PSS and the electrolyte and the resistance of PEDOT:PSS.

We then demonstrate that the characteristic time is sensitive to the concentration of dopamine (DA), a neurotransmitter of the family of catecholamines involved in cell signalling[9]. DA deficit is a hallmark of Parkinson's disease, due to the degeneration of dopaminergic neurons[10]. In physiological environment DA is in its cationic form, hence it can interact with PEDOT:PSS and modulate the conductivity through both π-π interaction, endowed by the presence of aromatic rings, and a cation-π interaction, due to the ammonium group[11]. The modulation of conductivity is reflected by the dependence of τ, extracted from the STP characterization of the device, on the concentration of DA. Our detection mechanism is shown to successfully discriminate DA from its physiological interfering agent, ascorbic acid (AA), which is an anion and hence interacts with PEDOT:PSS in a different manner.

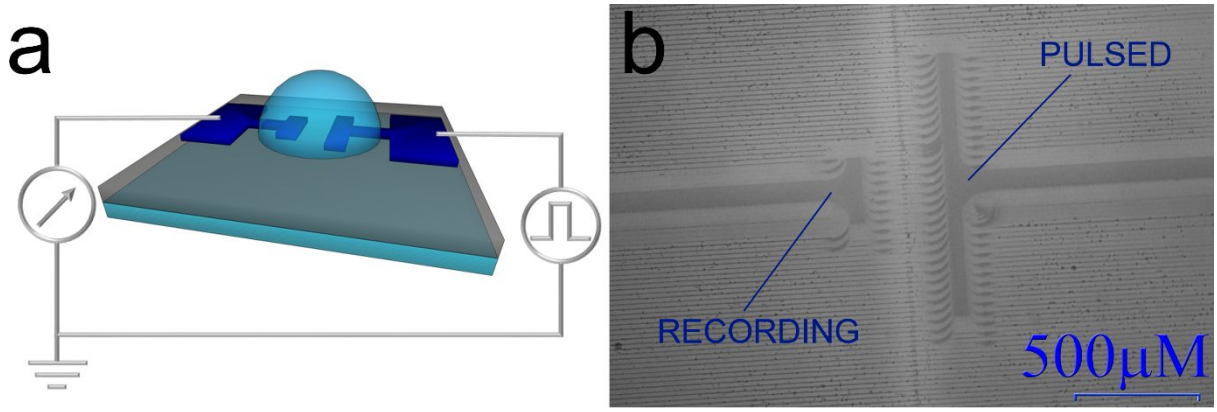

Figure 1: Schematic layout (a) and optical micrography (5X) (b) of the whole organic device in which are highlighted the two different geometries for the pulsed and the recording electrodes.

2. EXPERIMENTAL SECTION

2.1 Fabrication of the organic synapses

Organic synapses were fabricated according to the layout of Fig.1a. The flexible substrate is Polydimethylsiloxane (PDMS). PDMS and its curing agent (Sylgard 184, Dow Corning, Midland, USA) were mixed in 10:1 ratio, degassed in vacuum in order to eliminate trapped air bubbles, then spin casted on a glass substrate. The glass support was treated with Hexamethyldisilazane (HMDS) vapor overnight before spin coating. PDMS was spin coated at 500 rpm for 180 s (acceleration 500 rpm/s), and then cured in a standard thermostatic oven for 1h at 120 °C. The resulting PDMS film (approximately 100 μm high) was treated with N_2 plasma, and then PEDOT:PSS suspension (Clevios™ PH1000) with

added 0.2% Glymo (3- glycidoxypropyltrimethoxysilane) and 5% DMSO was spin coated and then cured at 120 °C for 20 minutes in a oven. PEDOT:PSS electrodes were patterned by means of a short-pulsed Nd:YAG infrared (IR)-laser (centre wavelength λ=1064 nm) with a laser scan marker (ScribaR, Scriba Nanotecnologie S.r.l, Bologna, Italy)[12]. A Computer Aided Design (CAD) of the electrodes was uploaded in the control software and then transferred on the substrate. Fig.1b shows an optical micrography of the substrate after the patterning; both the electrodes and the traces left by the laser (darker parallel lines) are visible. The pulsed electrode is made larger in order to decrease its impedance and hence to enhance the intensity of the capacitive current. The recording electrode is made smaller in order to enhance the density of charges in the electric double layer, and hence amplify the signal to noise ratio.

2.2 Electrical measurements

Electrical measurements have been performed in a buffer solution, Phosphate Buffered Saline (PBS) 50 mM, pH 7.4 in order to mimic physiological conditions. All measurements were carried out in atmosphere conditions (temperature and humidity). The pulsed square waves were designed and controlled by a custom-built control suite software. The two electrodes were connected to an Agilent B2912A Source Meter Unit according to the scheme depicted in Fig.1a. The measurements were carried out in a low-noise configuration (4 pA of base noise level). Recordings were started after an initial buffer time of 180 s, in order to start from a steady-state condition.

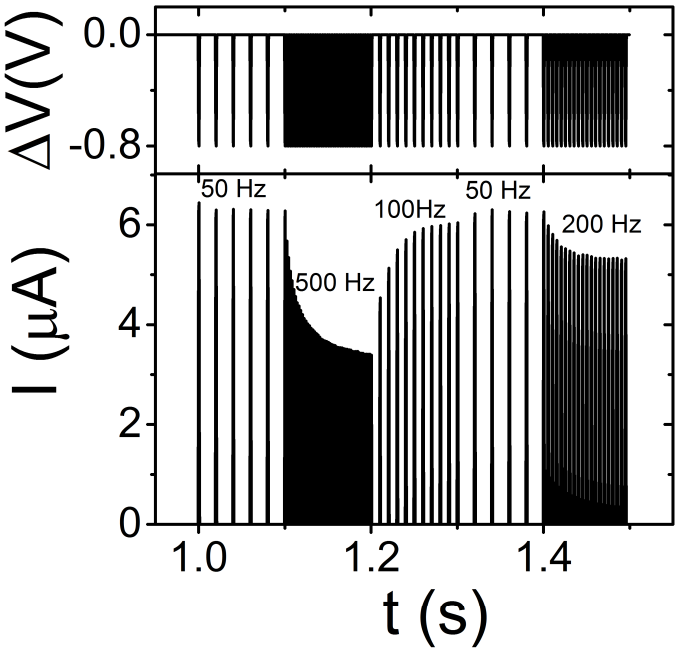

Figure 2: Typical STP response of the device to impulses at different frequencies (see top) and the corresponding current responses (bottom). Depressing behavior is observed at the highest frequencies (i.e. 500 Hz and 200 Hz).

3. RESULTS AND DISCUSSIONS

The whole organic artificial synapses showed a robust and reproducible STP response throughout a wide range of pulse amplitude and frequency as shown in Fig. 2. Different pulse trains were tested, changing frequency and pulse amplitude, in order to maximize the dynamic response of the depressing region of the STP. This optimization led to the development of a fast and effective protocol for operating the synapse as a sensor exclusively under suppressing behavior[6,7]. The protocol contemplates one second of buffer time followed by one second of square wave stimulation at 500Hz, with pulse amplitude as low as 200mV. This protocol was applied to devices in electrolytic solutions containing

increasing concentration of DA and AA, starting from 50nM up to 500µM.

Evolution of the suppressing behavior in response to different analyte concentrations is shown in Fig. 3. Fig.3a and 3b show the response of the device by varying by two orders of magnitude the concentration of DA and AA, respectively; as regards DA a significant change of the response was observed, while the tracks recorded for AA are superimposable. These results hint that the decay timescale depends on the concentration of DA, and that there is no, or marginal, dependence on the concentration of AA. Furthermore, in Fig.3c the plot of the normalized current responses of devices exposed to DA and AA is shown. It appears that the decay of AA maxima is slower than the decay of DA. This means that the chemical nature of the analyte affects the decay rate of the synapse depressing behavior.

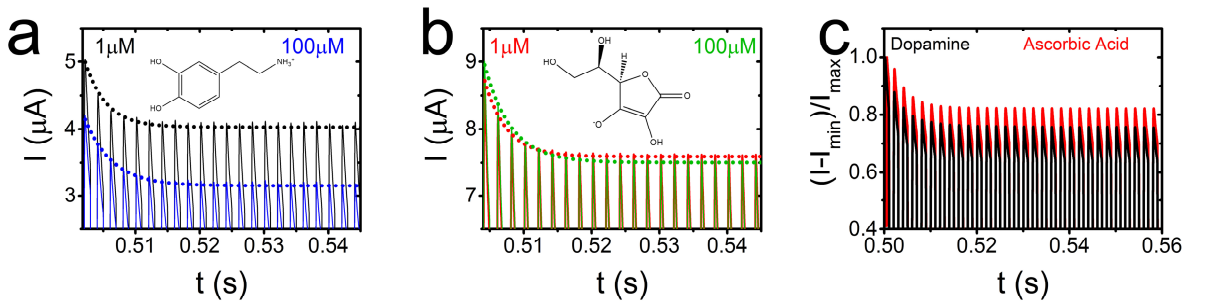

Figure 3: (a) STP current responses to a 500 Hz stimulation (depressing behavior) for 1 µM and 100 µM solutions of DA and (b) AA and fit curves (dotted lines) from eq 1. The current response changes at different DA concentrations (a), while it does not undergo a variation vs AA concentration (b). (c) Normalized current response for equal concentrations of DA and AA (viz. 250 µM).

In order to express quantitatively the evolution of the current *vs* characteristic time in response to the variation of analyte concentration, we extract the characteristic time of the suppressing behavior, τ as detailed in the following. First of all, the maximum current value I_n for each (n-*th*) spike was extracted from the STP characteristic and all the maxima were plotted vs time *t*. The observed trend of the maxima was then fitted according to:

$$I_n(t_n) = (I_0 - I_{DC}) \cdot \exp\left(-\frac{t_n}{\tau}\right) + I_{DC} \quad (1)$$

where I_0 is the magnitude of the current in response to the first voltage spike, and I_{DC} is the long-time (direct current DC) plateau that is asymptotically reached upon the exponential decay. Example of best fit curves are shown in Fig. 3 as dotted lines.

In Fig.4 the dose-response curves are shown. Fig. 4a shows the correlation between τ and DA concentration. The observed strong dependence indicates how the characteristic time τ of the PEDOT:PSS/DA system substantially changes upon increasing DA concentration. Changes of τ can be ascribed to the increased impedance of the system, due to the cation-π interaction that immobilizes positive charges in the polymeric PEDOT:PSS network thus lowering its conductivity and leading to the progressive neutralization of the sulfonate anions. The dose-response curve was fitted according to equation 2, and the result of the fit is shown as solid blue line in Fig.4a.

$$\tau = \tau_0 + \tau_\infty \left(1 - e^{-\left(\frac{[DA]}{\xi}\right)^\beta}\right) \quad (2)$$

Here the exponent β indicates the steepness of the rise in the lower concentration range, τ_∞ is the asymptotic plateau corresponding to the upper detection limit of the sensor, τ_0 is the intrinsic τ value when no DA is present in solution, ξ is the concentration of DA corresponding to the crossover from rising branch to the plateau. The inset of Fig. 4a highlights

the "power-law" trend implicit in eq. 2, since the first non-zero expansion term of the factor in parenthesis of Eq. 2 is proportional to $[DA]^{\beta}$.

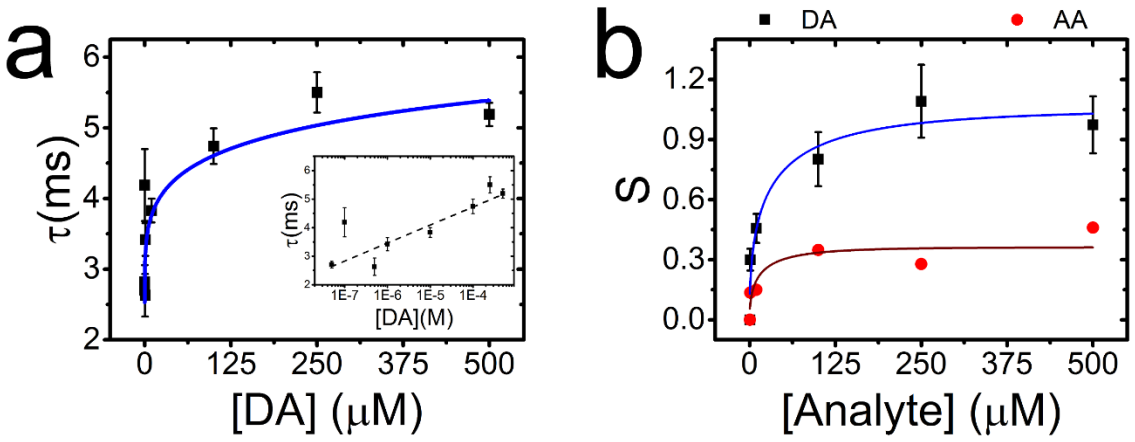

Figure 4: (a) τ values extracted at different DA concentrations (i.e. from 0 to 500 μM). The blue curve is the best fit obtained with function eq. 2; the inset shows the lin-log dependence of τ on [DA]. (b) S variation for same concentrations of DA (black squares) and AA (red circles, error bars are comparable to the marker size); continuous lines are the best fits obtained with function eq. 3.

In order to suppress device-to-device variation, a normalization of τ has been operated adapting a method originally developed by Ishikawa et al.[13], to yield a signal variation $S = \frac{\tau - \tau_0}{\tau_0}$ which results to be robust from device to device. Its dependence on [DA] can be fitted as follows:

$$S = \frac{\tau_\infty}{\tau_0}\left(1 - e^{-\left(\frac{[DA]}{\xi}\right)^{\beta}}\right) \tag{3}$$

Comparison of S vs [Analyte] plots for DA and AA and their respective fits are shown in Fig.4b. It evidences the sensitivity of the artificial synapse and the specificity towards DA vs AA. In Table 1 the comparison of the best-fit parameters ξ, β, and τ_∞/τ_0 is reported.

Table 1. Best fit parameters for S vs [Analyte].

Analyte	β	ξ **(μM)**	τ_∞/τ_0
Dopamine	0.49 ± 0.18	32 ± 12	1.05 ± 0.18
Ascorbic Acid	0.52 ± 0.23	22 ± 17	0.38 ± 0.04

It is important to notice how ξ and β values are not statistically different, while τ_∞/τ_0 more than doubles from AA to DA. We may argue that both ξ and β are characteristic of the device, while τ_∞/τ_0 is strongly related to the PEDOT:PSS/Analyte interaction.

It is possible to infer that the two possible pathways of interaction between PEDOT:PSS and DA (i.e. cation-π and π-π) influence constructively the resistance of PEDOT:PSS electrodes and, subsequently, the τ of the device. This does not seem to occur in the case of AA, which may interact only by π-π interaction. The negative charge of AA is repelled by PSS^- which, according to studies of the micromorphology of PEDOT:PSS, is exposed to the electrolyte, whereas PEDOT

forms the core of the domains. This may cause the PEDOT:PSS to be also ion-charge selective, which enhances the discrimination of the two species.

The sensitivity, being the derivative of the function S Eq. 3 with respect to the analyte concentration, in the case of DA will read:

$$\frac{dS}{d[DA]} = \frac{\beta}{[DA]} \frac{\tau_\infty}{\tau_0} \left(\frac{[DA]}{\xi} \right)^\beta e^{-\left(\frac{[DA]}{\xi}\right)^\beta} \tag{4}$$

The curves in Fig. 5, obtained from Eq. 4, show that the sensitivity is much higher at lower concentrations, and that it scales as τ_∞/τ_0 at each concentration. At the physiological/pathological levels of DA (hundreds of nM to few nM), the latter have not been explored in this work, the sensitivity is estimated to be on the order of 5 10^5 mol^{-1}. Because the physiological concentration of AA in the body is on the order of µM vs nM concentration of DA, we expect that our device will be sensitive and selective to DA in physiological conditions, being the sensitivity for DA more than 200 times larger than the one for AA at their respective physiological levels. The sensitivity should be even higher at pathological levels of DA (low nM). This sensitivity towards DA greatly in excess of the sensitivity of AA is indeed responsible for the selectivity of our device, and supports the preferential interaction of DA vs AA towards PEDOT:PSS.

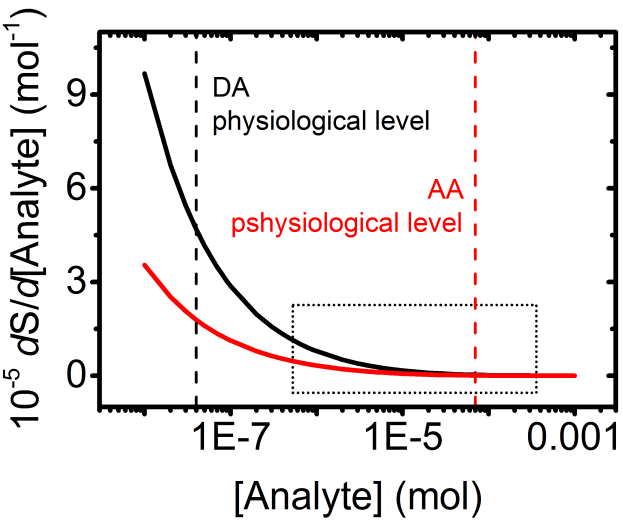

Figure 5: plots of the theoretical sensitivity from eq. 4 calculated with best-fit parameters of the curve in 4b (corresponding to the eq. 3) for DA (black) and AA (red). In the graph the average physiological levels of the two analytes are highlighted with dashed lines (black and red respectively), the dotted rectangle highlights the concentration range for which the comparison has been experimentally evaluated (see fig. 4b).

The possibility to discriminate DA from AA by exploiting different interactions of the analyte with the active material is extremely attractive. The standard fast-scan cyclic voltammetry characterization does not allow one to resolve the two species, being the redox potentials of the two species close to each other. There, the sensitivity is ≈ 10^8 mol^{-1} [14]. Their discrimination requires a separation that may be implemented with an ion-selective nafion coating of the electrode. Our organic synapse has the advantage that it integrates both the electrical transduction and the ion selectivity through the multifunctionality of PEDOT:PSS. These results herald PEDOT:PSS as a promising material for dopamine, and possibly other catecholamines, ultra-high sensitive detection.

4. CONCLUSIONS

A whole organic artificial synapse has been presented. It was fabricated by patterning PEDOT:PSS electrodes on PDMS that are biased in frequency to yield a frequency dependent STP response. The timescale of the response is shown to be sensitive to the concentration of DA, a neurotransmitter relevant for the monitoring of Parkinson's disease. In particular, the characteristic time of the synapse, τ, increases as power law with the concentration of DA in solution. The sensitivity of the sensor towards DA has been validated comparing signal variation in the presence of DA and its principal interfering agent, AA. The synapse appears ultra sensitive to DA and selective thanks to a more specific cation-π interaction. The whole organic synapse, being biocompatible, soft and flexible, is attractive for implantable devices aimed to real-time monitoring of DA concentration in bodily fluids, to be used as a diagnostic tool, for instance, in chronic neurodegenerative diseases such as Parkinson's disease.

Acknowledgements

This work was funded by the EU 7th Framework Programme [FP7/2007–2013] under Grant Agreement No. 280772, "Implantable Organic Nanoelectronics (I-ONE-FP7)" project and IT MIUR Bilateral Project IT/SE "Poincaré" (Con il contributo del Ministero dell'Istruzione dell'Università e della Ricerca della Repubblica Italiana).

REFERENCES

[1] Palazzo, G., De Tullio, D., Magliulo, M., Mallardi, A., Intranuovo, F., Mulla, M. Y., Favia, P., Vikholm-Lundin, I., Torsi, L., "Detection Beyond Debye's Length with an Electrolyte-Gated Organic Field-Effect Transistor," Adv. Mater. **27**(5), 911–916 (2015).

[2] Casalini, S., Leonardi, F., Cramer, T., Biscarini, F., "Organic field-effect transistor for label-free dopamine sensing," Org. Electron. **14**(1), 156–163, Elsevier B.V. (2013).

[3] Casalini, S., Dumitru, A. C., Leonardi, F., Bortolotti, C. A., Herruzo, E. T., Campana, A., de Oliveira, R. F., Cramer, T., Garcia, R., et al., "Multiscale Sensing of Antibody–Antigen Interactions by Organic Transistors and Single-Molecule Force Spectroscopy," ACS Nano **9**(5), 5051–5062 (2015).

[4] Khodagholy, D., Gelinas, J. N., Thesen, T., Doyle, W., Devinsky, O., Malliaras, G. G., Buzsáki, G., "NeuroGrid : recording action potentials from the surface of the brain," Nat. Neurosci. **18**(2), 310–316 (2014).

[5] Ruppert, E.E., Fox, R.S., Barnes, R.D. [Invertebrate Zoology: A Functional Evolutionary Approach, 7th Edition], Cengage Learning, 978-0030259821.

[6] Alibart, F., Pleutin, S., Guérin, D., Novembre, C., Lenfant, S., Lmimouni, K., Gamrat, C., Vuillaume, D., "An Organic Nanoparticle Transistor Behaving as a Biological Spiking Synapse," Adv. Funct. Mater. **20**(2), 330–337 (2010).

[7] Desbief, S., Di Lauro, M., Casalini, S., "Electrolyte-gated organic synapse transistor interfaced with neurons," Org. Electron. **38**, 21–28, Elsevier B.V (2016).

[8] Gkoupidenis, P., Schaefer, N., Garlan, B., Malliaras, G. G., "Neuromorphic Functions in PEDOT:PSS Organic Electrochemical Transistors," Adv. Mater. **27**(44), 7176–7180 (2015).

[9] Iversen, S. D., Iversen, L. L., "Dopamine: 50 years in perspective," Trends Neurosci. **30**(5), 188–193 (2007).

[10] Michel, P. P., Hirsch, E. C., Hunot, S., "Understanding Dopaminergic Cell Death Pathways in Parkinson Disease," Neuron **90**(4), 675–691 (2016).

[11] Dougherty, D. A., "The cation-π interaction," Acc. Chem. Res. **46**(4), 885–893 (2013).

[12] Campana, A., Cramer, T., Greco, P., Foschi, G., Murgia, M., Biscarini, F., "Facile maskless fabrication of organic field effect transistors on biodegradable substrates," Appl. Phys. Lett. **103**(7), 0–4 (2013).

[13] Ishikawa, F. N., Curreli, M., Chang, H., Chen, P., Zhang, R., Cote, R. J., Thompson, M. E., Zhou, C., "A Calibration Method for Nanowire Biosensors to Suppress Device-to-Device Variation," ACS Nano **3**(12), 3969–3976 (2009).

[14] Bucher, E. S., Wightman, R. M., "Electrochemical Analysis of Neurotransmitters," Annu. Rev. Anal. Chem. **8**(1), 239–261 (2015).